Hybrid Photopatterned Enzymatic Reaction (HyPER) for in Situ Cell Manipulation

Donald R. Griffin,[a] Jacob Borrajo,[a] Allyson Soon,[a] Giovanny F. Acosta-Vélez,[a] Victor Oshita,[a] Nicole Darling,[a] Julia Mack,[c] Thomas Barker,[b] M. Luisa Iruela-Arispe,[c] and Tatiana Segura*[a]

The ability to design artificial extracellular matrices as cell-instructive scaffolds has opened the door to technologies capable of studying the fate of cells in vitro and to guiding tissue repair in vivo. One main component of the design of artificial extracellular matrices is the incorporation of biochemical cues to guide cell phenotype and multicellular organization. The extracellular matrix (ECM) is composed of a heterogeneous mixture of proteins that present a variety of spatially discrete signals to residing cell populations. In contrast, most engineered ECMs do not mimic this heterogeneity. In recent years, photo-deprotection has been used to spatially immobilize signals. However, this approach has been limited mostly to small peptides. Here we combine photo-deprotection with enzymatic reaction to achieve spatially controlled immobilization of active bioactive signals that range from small molecules to large proteins. A peptide substrate for transglutaminase factor XIII (FXIIIa) was caged with a photo-deprotectable group, which was then immobilized to the bulk of a cell-compatible hydrogel. With focused light, the substrate can be deprotected and used to immobilize patterned bioactive signals. This approach offers an innovative strategy to immobilize delicate bioactive signals, such as growth factors, without loss of activity and enables in situ cell manipulation of encapsulated cells.

Introduction

Advances in developmental, cell, and molecular biology are beginning to map out the spatial and temporal regulation of the bioactive and physical signals required for the orchestration of tissue formation.[1] This spatial regulation of bioactive signals is most dramatic during embryogenesis, in which a whole organism is created from just one cell. However, the fine-tuned orchestration of tissue formation also occurs in adults during homeostasis and to allow wound healing. It is clear from the wealth of literature that one signal and one static environment are not sufficient for tissue formation or homeostasis. Thus, our ability to probe the fate of human cells in vitro and determine the minimum required signals for tissue formation or to promote a desired cell phenotype is limited by our inability to create cellular microenvironments with complex and dynamic patterns of signals.

Engineered extracellular matrices (eECMs) aim to bridge the gap between in vivo studies and those performed in tissue culture plastic. eECMs can be developed through the use of synthetic polymers or the modification of existing natural polymers.[2, 10] Studies in eECMs have opened the door to understanding how changes in the bulk physical and chemical characteristics of these three-dimensional environments influence tissue formation,[3] stem-cell differentiation,[10] pathological conditions,[2a, b] and drug delivery.[4] Although eECMs have enabled us to study the behavior of cells in an environment closer to what they experience in vivo, most still fail to recreate the heterogeneous nature of the natural ECM both in spatial control of the signal placement and in temporal control of signal availability.

To introduce heterogeneity, several approaches using light-controlled platforms to modify the physical and chemical properties of hydrogels have been explored. Light-based platforms can allow for modifications ranging from the bulk to micrometer-sized resolution ($< 10\ \mu$m) due to the high level of control available for the stimulus. These platforms fall into two basic modes: subtraction or addition. Photolytic "subtraction" strategies depend on breaking a covalent bond to either decrease hydrogel crosslinking density (physical) or release an attached signal (chemical).[5] The Anseth group used this strategy to control the growth of encapsulated mesenchymal stem cells.[5b] Subtractive methods are difficult to use for generating precise spatially limited chemical patterns, primarily due to the large

[a] Dr. D. R. Griffin, J. Borrajo, Dr. A. Soon, G. F. Acosta-Vélez, V. Oshita, N. Darling, Prof. T. Segura
Department of Chemical and Biomolecular Engineering
University of California, Los Angeles
420 Westwood Plaza, Los Angeles, CA 90095 (USA)
E-mail: tsegura@ucla.edu

[b] Prof. T. Barker
Department of Biomedical Engineering
Georgia Institute of Technology and Emory University
315 Ferst Dr, Atlanta, GA 30332 (USA)

[c] Dr. J. Mack, Prof. M. L. Iruela-Arispe
Department of Molecular, Cellular, and Developmental Biology
University of California, Los Angeles
128 Hershey Hall, Los Angeles, CA 90095 (USA)

quantity of deprotection needed to eliminate unwanted signal. In contrast, the "addition" mode only presents the desired signal in the areas exposed to light. Previous additive methods have relied on either the activation of photopolymerizable groups (e.g., acrylates) or the uncaging of protected thiols for controlled Michael-type reactions. One of the more successful techniques, employed by the Shoichet group, has allowed the attachment of multiple proteins within hydrogel matrices.[5d] Beyond this exception, the vast majority of additive strategies have focused on the addition of small oligopeptides. The absence of complex signal patterning is not surprising, as the use of more complex signals (e.g., growth factors) is limited by molecule stability during synthetic modification and purification, as well as the possibility of decreased signal activity as a result of modification and immobilization onto the scaffold. A less explored approach to pattern signals into hydrogel scaffolds is the use of protected peptides that are substrates for enzymes, such that no enzymatic activity is observed in the presence of the protective group, but, upon light exposure, the enzyme can recognize the peptide. This approach was first explored by using caged peptide substrates for caspases.[6] Upon photo-deprotection and enzymatic digestion of the light-exposed areas, the free amine resulting from the digestion was used to immobilize RGD or biotin. Although this report only demonstrated two-dimensional patterning and used the technology for cell-sorting rather than tissue-regeneration applications, it demonstrated the ability to use caged peptides to control enzymatic activity within hydrogel scaffolds.

Herein we present a novel approach, termed hybrid photo-patterned enzymatic reaction or HyPER, to immobilize bioactive signals with spatial control into cell-compatible hydrogel scaffolds. Our platform uses an activated transglutaminase factor XIII (FXIIIa)-catalyzed reaction to immobilize signals to light-activated regions of the hydrogel. To control enzymatic activity, we employ a caged enzyme substrate that is immobilized to the backbone of the hydrogel matrix. The cage prevents enzymatic attachment of the signal before light exposure. Following localized removal of the light-sensitive cage, FXIIIa catalyzes the formation of a stable amide bond between the desired bioactive signal and the hydrogel backbone.

Results and Discussion

FXIIIa chemistry and HyPER

FXIIIa is an important enzyme in the blood-coagulation cascade and is partially responsible for clot stability through the introduction of additional covalent bonds.[7] Building from this natural capacity, FXIIIa has previously been used for crosslinking and bulk biomolecule immobilization within hydrogels.[8, 10] More specifically, FXIIIa catalyzes the formation of a stable non-canonical amide bond between the ε-amine of lysine and the γ-carboxamide of glutamine. For our platform, the FXIIIa-associated lysine is contained within an oligopeptide, Ac-FKGGERCG-NH2[8d] (or K peptide), which includes a cysteine to allow pseudo-Michael-addition attachment to any hydrogel

backbone polymer modified with a suitable vinyl group (Figure 1A). The FXIIIa-associated glutamine is associated with the bioactive signal to be immobilized and is contained within the peptide sequence NQEQVSPL[8a, 9] (or Q peptide). Both of these sequences were previously identified to be either a synthetic substrate for transglutaminase (K peptide) through a rational peptide library[8d] or identified as a natural substrate for FXIIIa, and have been previously used to form hydrogel scaffolds[8c, d] or to immobilize bioactive signals within them.[8a, b, 9, 10]

Caged K peptide substrate synthesis

To allow photopatterning, we caged the ε-amine of lysine with a photoactive *ortho*-nitrobenzyl (*o*-NB) vanillin derivative, 4-(4-formyl-2-methoxy-5-nitrophenoxy)butanoic acid.[11] The *o*-NB cage prevents the FXIIIa-catalyzed attachment of the glutaminyl peptide residue in the Q peptide. The *o*-NB cage was chosen for its high absorption spectra ($\lambda_{peak} \sim 350$ nm) and fast degradation time ($t_{1/2} \sim 7$–8 min at 10 mW cm^{-2}),[11, 12] thus minimizing the risk of damage to present biomolecules (e.g., DNA). In addition, *o*-NBs are susceptible to multiphoton degradation, thus allowing for true 3D patterning within hydrogels.[5b, c] Once the cage is removed through photo-deprotection, the lysine returns to a primary amine capable of transglutaminase modification (Figure 1A).

The *o*-NB molecule was synthesized from vanillin. Briefly, we etherified vanillin through a Williamson etherification with ethyl-4-bromobutyrate. This is followed by nitration at the *ortho*-position with nitric acid to provide light sensitivity. The nitrated product was hydrolyzed with trifluoroacetic acid to produce a more water soluble material before being treated with the full-length peptide (Figure 1B). We caged the ε-amine residue of the K peptide through reductive amination, using picoline borane to directly modify the full-length peptide in a single reaction that results in a high yield (40–50%) following preparatory HPLC purification of the caged peptide. The absence of unmodified K peptide and the overall purity of the product were verified by ESI-MS (see the Supporting Information).

Caged K peptide photo-deprotection kinetics and FXIIIa immobilization can be predicted

To determine the extent to which we could predict the amount of signal that would be immobilized following photo-deprotection and FXIIIa-mediated immobilization, we first explored the kinetics of light-controlled uncaging of the protected K peptide in a soluble model system. Caged K peptide was exposed to 365 nm filtered UV light ($I = 20$ mW cm^{-2}). At different exposure times, samples ($n = 3$) were analyzed for the presence of free amines on the uncaged lysine residues through treatment with trinitrobenzene sulfonate (TNBS), a common assay for primary amine quantification[13] (Figure 1C). Using a simplified equation for exponential degradation[14] [Eq. (1)], we determined the intensity dependent degradation constant of the caged K peptide, $k = 0.00024$ mW^{-1} cm^2 s^{-1}, which is comparable to previously published results of *o*-NB groups
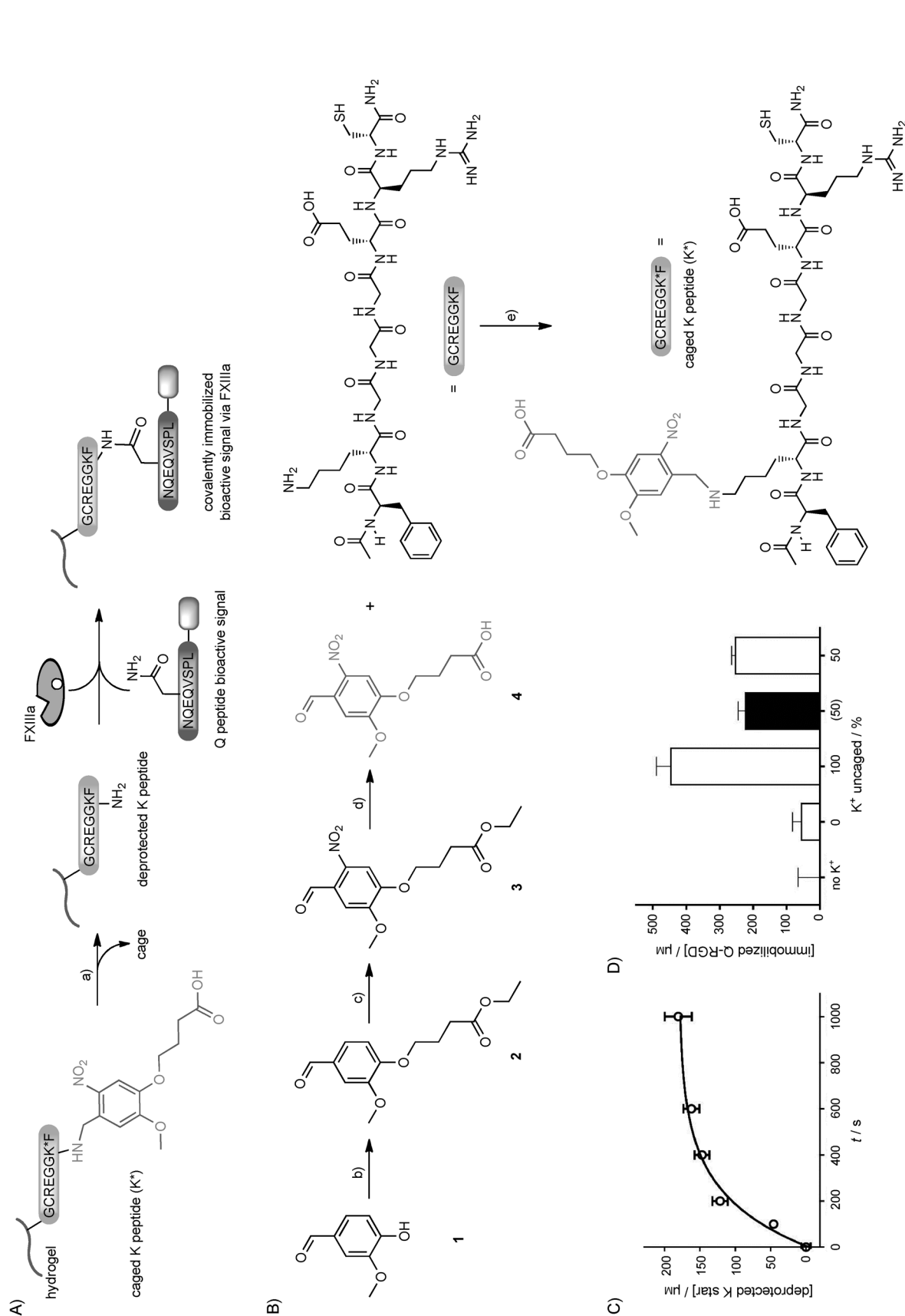
Figure 1. HyPER achieves predictable immobilization kinetics. A) HyPER utilizes a caged peptide substrate for FXIIIa (K* peptide) that prevents FXIIIa activity unless the substrate has been deprotected by exposure to light at 365 nm. This allows for site-specific deprotection of the K* peptide. Following deprotection, the bioactive signal can be immobilized by adding the second substrate for FXIIIa to it and incubating the K peptide-modified hydrogel, the Q peptide bioactive signal and FXIIIa. a) Photodeprotection, 365 nm light, 10 mWcm^{-2}. B) Synthesis of the photocaged group and direct peptide modification. b) Ethyl-4-bromobutyrate, K$_2$CO$_3$, DMF, overnight, >90%; c) HNO$_3$, 0°C→RT, 4 h, >60%; d) TFA, H$_2$O, 90°C, 2 h, >90%; e) picoline borane complex, MeOH/CH$_3$CO$_2$H (10:1), 40–50%. C) K* peptide photo-deprotection kinetics. D) FITC-Q-RGD was immobilized to hydrogels with either 100 or 50% deprotection of K* by using FXIIIa. The amount bound for 50% was half that for 100% deprotection (matching the predicted value, shown in black); this indicated that photo-deprotection and bioactive signal conjugation can be predicted.

derived from vanillin ($k = 0.00015$, 0.00026).[11,12] At 20 mW cm^{-2}, this degradation constant results in a $t_{1/2}$ of ~208 s, which can be increased by lowering the light intensity (e.g., 10 mW cm^{-2}: $t_{1/2} = 416$ s) or vice versa.

$$[K] = [K^*]_0(1 - e^{-klt}) \tag{1}$$

k = exponential constant, l = intensity, t = time.

We wanted next to determine if, with a defined degradation constant, we could predict the amount of bioactive signal immobilized through FXIIIa in a cell-compatible hydrogel. To determine the predictability of the system, we ran an immobilization test within a hyaluronic acid-based (HA) hydrogel (1.6 mм caged K peptide, K*) using a fluorescently tagged Q-RGD substrate and measuring depletion of surrounding fluorescence to determine immobilization (Figure 1D). This HA hydrogel has been extensively used in our laboratory[3a,4,15] for the culture of stem cells and is synthesized through Michael-type addition of acrylates present in the HA backbone and dithiol-containing peptides. One set of hydrogels was fully uncaged (l = 20 mW cm^{-2}, $t = 1200$ s), while a second was exposed to enough light to theoretically achieve 50% uncaging (l = 10 mW cm^{-2}, $t = 416$ s). Both samples were exposed to FXIIIa and FITC-Q-RGD for conjugation. The fully uncaged gels displayed (0.446 ± 0.085) mм Q peptide immobilized, thus we expect the 50% uncaged set to display ~(0.223 ± 0.042) mм Q peptide, which is what we observed: (0.253 ± 0.024) mм (Figure 1D). However, with an efficiency of only 27.2%, this also demonstrated that, even with full deprotection, we could not achieve 100% utilization of the deprotected K peptides through FXIIIa chemistry. As controls, the same hydrogels were used with either no light exposure (0% uncaged) or no K peptide added but with FXIIIa. The unexposed hydrogel showed no statistically significant attachment of Q peptide over the control without K peptide and both controls were statistically lower than those exposed to light and containing both FXIIIa and K peptide. Thus, the predictable kinetics of deprotection and the FXIIIa-catalyzed reactions allow for predictable immobilization.

HyPER can achieve spatial co-immobilization of multiple bioactive signals under cell-compatible conditions

We next wanted to determine if we could use HyPER to immobilize bioactive signals of different molecular weight and complexity using either filtered 365 nm light or a two-photon confocal microscope. For these experiments, we used either four-arm PEG-vinyl sulfone (PEG-VS) or HA-acrylate (HA-AC) both crosslinked through Michael addition with dithiol-containing peptides. Our chosen substrates included an RGD adhesive peptide (Q-RGD), a fibronectin protein fragment (Q-FNIII9*-10),[2a,b,10] and two growth factors (vascular endothelial growth factor, Q-VEGF, and platelet-derived growth factor, Q-PDGF). The Q peptide sequence was introduced either during solid-phase peptide synthesis (for smaller peptides containing a bioactive signal) or by introducing the sequence at the N terminus of larger proteins prepared by using standard recombinant

protein cloning and expression techniques[8b] (see the Supporting Information).

For all these experiments, 1.6 mм K* peptide was immobilized to the hydrogel backbone, and FXIIIa enzyme was added to the hydrogel prior to gelation. The hydrogel was formed by using 4% HA and an r ratio (mol thiol per mol acrylate) of 0.6, which resulted in an elastic modulus of 300 Pa. We first used a mercury lamp at 10 mW cm^{-2} intensity in combination with a photomask to deprotect the desired 2D areas within the hydrogel (Figure 2A). The hydrogel was then exposed to the conjugation solution, which contained the bioactive signal to be immobilized. After conjugation, the hydrogel was washed to remove unbound material. We first used PEG-VS to immobilize the small molecule N-hydroxysuccinimide (NHS)-Alexa 556. This immobilization does not use the HyPER platform, rather it uses deprotected amines for conjugation (Figure 2B). These data show that deprotection is possible and efficient, and generates a free amine. Next, we used the HyPER platform to pattern a variety of substrates into hyaluronic acid hydrogels by FXIIIa-
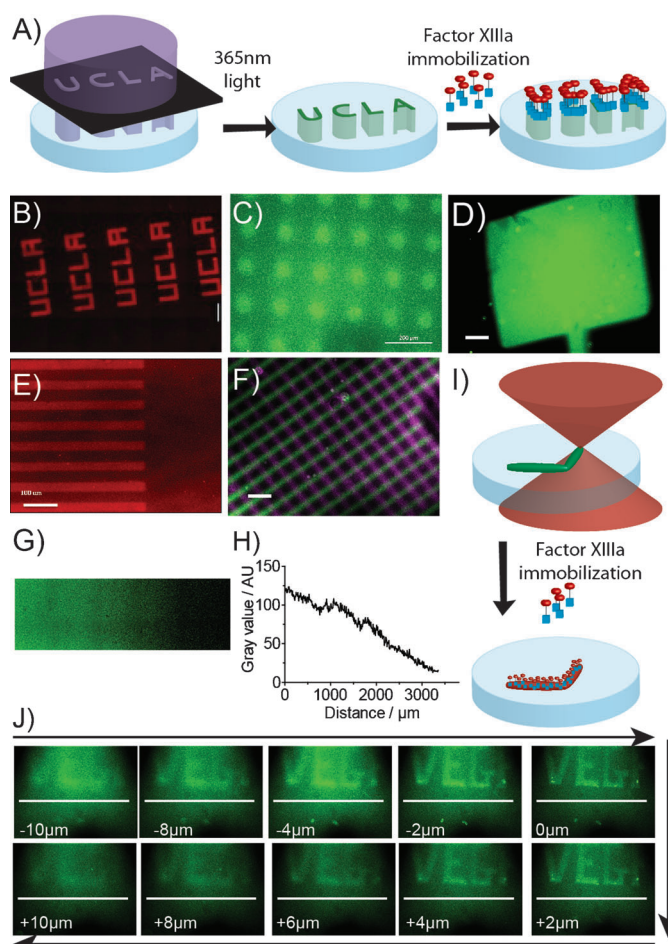

Figure 2. Immobilization of bioactive signals with different molecular weights by using HyPER. A) Schematic of HyPER immobilization of bioactive signals in hydrogel scaffolds by using a photomask. B)–D) Immobilization of Q-RGD (MW) in different patterns. E) Immobilization of an engineered fibronectin fragment FNIII9*10 (MW).[2a,b,10] F) Dual pattern of Q-RGD (purple) and Q-PDGF (green). G) Linear gradient of Q-RGD. H) Quantification of this linear gradient. I) Schematic of two-photon deprotection of K*-modified hydrogels. J) Two-photon patterning of RGD. Scale bars: 200 μm.

catalyzed immobilization. Using HyPER, we were able to immobilize fluorescently labeled Q-RGD in circles and a dumbbell, (Figure 2 C, D) and Q-FNIII9*-10 in lines (Figure 2 E) with 2D control over patterning.

We next wanted to determine if HyPER could achieve sequential immobilization of signals and immobilization in a gradient. We use the approach described above, except that, after photo-deprotecting and immobilizing Q-RGD in lines and washing the hydrogel, a second deprotection with 90° lines was performed followed by a second incubation with fluorescently labeled Q-PDGF. We were able to immobilize both bioactive signals (Figure 2 F), thus demonstrating that the FXIIIa enzyme remains active after the first modification and allows a second conjugation to take place. Dual-factor immobilization is essential for the generation of complex eECM environments because many bioactive signals are synergistic when placed in close proximity. In order to generate a continuous gradient, we used a neutral-density, continuous-gradient optics filter to pattern the hydrogel and immobilize Q-RGD (Figure 2 G). Converting the image to gray scale and determining pixel intensity as a function of distance quantified the gradient (Figure 2 H). Gradients are of great importance in biological systems as they have been shown to be major morphogenic signals during development,[16] adult healing,[17] and disease.[18]

In addition to 2D patterns, we tested the ability of our K* peptide to undergo multiphoton uncaging. Exposure to two-photon confocal microscopy has been previously shown to be able to deprotect o-NB groups, resulting in 3D controlled patterning.[5c, d] We used a similar strategy to that detailed above, except that uncaging was achieved by using a two-photon confocal microscope at 730 nm (twice λ_{peak}). Patterning was achieved by setting a region of interest (ROI) and performing multiple (~40) scans (Figure 2 I). Q-VEGF was immobilized in true 3D patterning (Figure 2 J), as shown by the depth dependence of the pattern focus area. The VEGF pattern was 180 μm wide and 75 μm high, with lettering as thin as 6 μm and an overall z-axis depth of ~20 μm.

The sharpness of the patterns can be improved by enhancing the accessibility of the K peptide

Although we were able to immobilize all the bioactive signals with spatial control by using HyPER, the pattern sometimes was not as sharp as we expected. As stated above, our current method only has 27.2% efficiency. We hypothesized that the reason for the low attachment was access of the K peptide substrate to the enzyme. To test this hypothesis, we gave the K* peptide a longer, more flexible arm from the HA backbone by modifying fewer of the molecules of HA (6.8% versus 100%) with the K* peptides (~50 K* peptides per modified HA molecule versus ~3.5 K* peptides per modified HA molecule). Visualization of FXIIIa-immobilized Q-RGD and Q-VEGF clearly demonstrates the increased binding when the K* peptide is immobilized in a clustered conformation, rather than homogeneous, gives a much sharper pattern with less background (Figure 3).
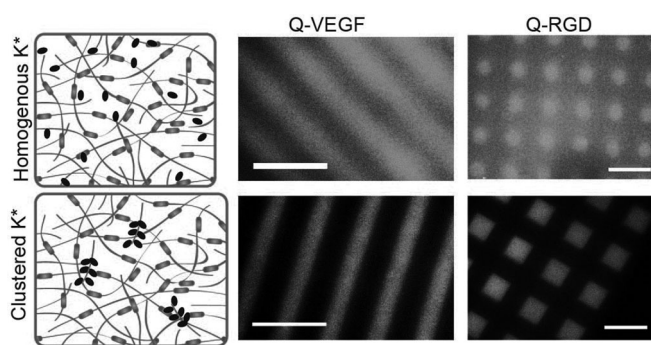

Figure 3. Clustering of K* peptide enhances the attachment of bioactive signals through HyPER. Cartoons show the concept of homogeneous (less attachment, less defined patterns, and higher background) and clustered K* peptide immobilization.

Using HyPER for in situ cell manipulation

We next wanted to determine if the immobilized bioactive signals are indeed active. We first tested whether RGD-modified gels resulted in cell attachment of mouse mesenchymal stem cells (mMSCs) to HyPER-modified hydrogels (Figure 4 A–F). K* peptide-modified gels were formed and were uniformly exposed to light (Figure 4 A, B) or not (Figure 4 C, D). We incubated both types of gels with the Q-RGD conjugation solution, with or without FXIIIa. Following conjugation, mMSCs were seeded on the surface of the gels, and phase images were taken at day 3. Only those cells that were cultured on fully exposed hydrogels with complete conjugation solution including FXIIIa resulted in significant spreading similar to our positive control, which contained RGD immobilized prior to hydrogel gelation as traditionally performed in our lab.[15] These results also illustrate the specificity of the FXIIIa reaction, with those gels that had light exposure but no FXIIIa resulting in no spreading (Figure 4 A). To determine if the cells could respond to a pattern or RGD, 100 μm circles of Q-RGD were patterned (Figure 4 G–I). mMSCs cultured on the surface of these gels showed self-organization into the patterned regions (Figure 4 I).

To investigate the bioactivity of immobilized Q-VEGF, increasing amounts of Q-VEGF were immobilized to K* peptide-functionalized hydrogels that were deprotected to achieve 0, 10, 40, and 80% deprotection. We expected that human umbilical vein endothelial cells (HUVECs) seeded on the VEGF-modified hydrogels would proliferate at different rates depending on the quantity of immobilized VEGF. Images taken at day 5, show that both 40 and 80% exposed samples (Figure 4 J, K) contain more cells than the 10 and 0% samples (Figure 4 L, M), thus supporting our expectations. Cell proliferation was quantified and showed similar proliferation rates for the 80 and 40% deprotected samples, but a statistically higher proliferation compared to 0 and 10% deprotected samples (Figure 4 O), thus indicating that different amounts of VEGF can be immobilized on the surface and that lower Q-VEGF immobilization results in lower proliferation. Interestingly, our negative control (no light exposure, 0% deprotected K*, Q-VEGF conjugation solution minus FXIIIa) resulted in more cell proliferation than the same
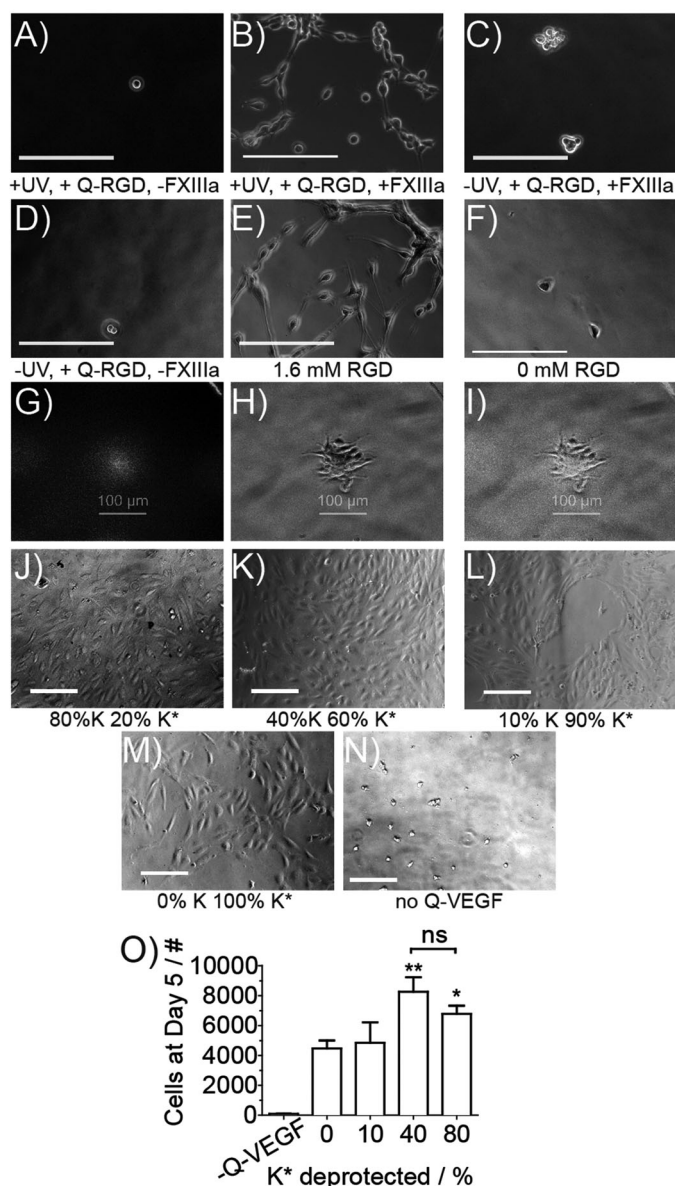
Figure 4. Bioactive signals immobilized through HyPER retain their activity. A)–F) mMSCs were seeded on the surface of Q-RGD-modified surfaces under the conditions given beneath each image. Only when light exposure is combined with Q-RGD and FXIIIa (B) do cells spread as well as when RGD is introduced to the bulk of the hydrogel (E). G) RGD patterned in 100 μm circles. H) Cells cluster to the location of the pattern. I) Overlay of the pattern and cell cluster. J)–M) HUVECs were cultured on the surface of Q-VEGF-modified hydrogels. Hydrogels were treated with decreasing amounts of light to result in 80 to 0% deprotection, and Q-VEGF was immobilized by using HyPER. 80 and 40% deprotection resulted in more cells at the cell surface than 10 or 0%. N) Cells did not display normal morphology on the "no Q-VEGF" control. O) Quantified HUVEC proliferation. Statistical analysis was performed by using an ANOVA with a Tukey post-test. Significance: *$p < 0.05$, and **$p < 0.01$.

surfaces not exposed to Q-VEGF. This result indicates that Q-VEGF has some affinity for hyaluronic acid that results in some background VEGF binding.

Finally, we wanted to explore the ability to pattern bioactive signals in situ in the presence of cells. For these experiments, HA-RGD-K* peptide hydrogels were synthesized with mMSCs, and FXIII was plated throughout the hydrogel volume. To de-

termine if HyPER was cell biocompatible, we performed a Q-RGD attachment and a LIVE/DEAD stain one day post HyPER (Figure 5 A–C). Cells that were exposed to light and subjected to the conjugation solution (thrombin, Q-RGD, Ca^{2+}) had the same level of LIVE cells as those that were not exposed to light but still had the conjugation solution, and as cells that did not have exposure to light or conjugation solution. This result shows that neither exposure to light nor the conjugation solution affect cell viability. We next wanted to look for a cellular response as a function of immobilized Q-PDGF. mMSCs have been shown to respond to PDGF.[19] The RGD peptide was bound by using Michael addition, and the cells were allowed to spread for one day before the K* was deprotected by full exposure (no pattern) to light or exposure through an optical filter gradient (365 nm light at 10 mW cm^{-2}). Q-PDGF was then FXIIIa-immobilized by using the same approach as shown in Figure 2, and the cells were further cultured for another two days before imaging. The cells cultured with the immobilized Q-PDGF gradient were found to have a different morphology and actin cytoskeletal staining than those cells cultured in homogenously bound or in the presence of soluble Q-PDGF (Figure 4 D–I). Comparing mMSCs cultured in homogenous, immobilized Q-PDGF (Figure 4 D, G) and in the presence of soluble Q-PDGF (Figure 4 F, I) to mMSCs cultured in PDGF immobilized in a gradient (Figure 4 E, H), we observed more polarized and extended cells among those cultured in the gradient than those cultured in the homogeneous hydrogels or exposed to soluble PDGF. This experiment highlights the types of experiments that could be performed with HyPER. One could plate
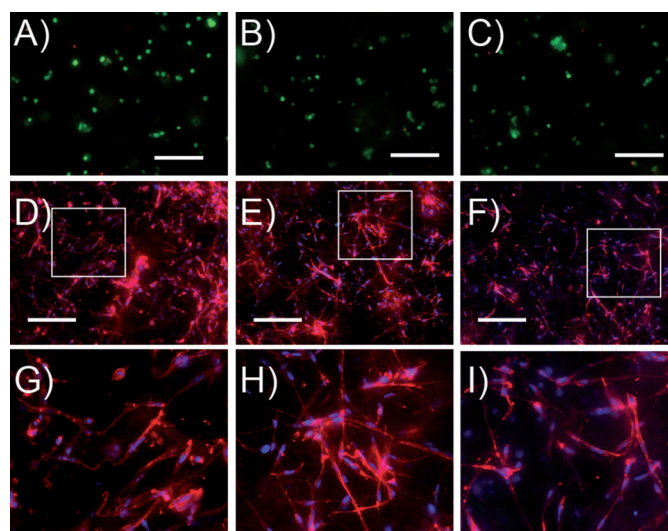

Figure 5. In situ cell manipulation by using HyPER. A)–C) Live/dead analysis of mMSCs within PEGVS gels with 1.6 mM caged K peptide. Cells showed high viability whether they were exposed to 365 nm light with (A) or without (B) application of Q-RGD, as did the sample left unexposed to either (C). D)–I) In situ hydrogel patterning of Q-PDGF in the presence of cells was performed by first making HA-RGD hydrogels with mMSCs plated homogeneously, and 24 h later immobilizing Q-PDGF homogeneously in the hydrogel through complete photo-deprotection (left) or deprotecting in a radial gradient (center). For comparison, mMSCs seeded inside HA-RGD gels were exposed to soluble Q-PDGF (right). Images in the bottom row are enlargements of the boxed regions directly above.

individual cells, cell clusters, organoids, etc. in the gel, then, after a planned period of time, a desired signal with the desired pattern can be immobilized to study the effect of that signal on morphogenesis or stem cell differentiation. This type of cell-biocompatible and protein-compatible patterning is not currently available.

Conclusions

In summary, we have developed a high-yield method for directly caging a FXIIIa-recognized substrate, K peptide. Using light, we were able to deprotect the FXIIIa substrate and then use FXIIIa to catalyze the immobilization of bioactive signals. Our studies have shown that the resultant platform displays quantifiable uncaging behavior that results in predictable immobilization behavior. The highly modular nature of the enzymatic immobilization chemistry allows for spatially defined patterns of a wide variety of active signals, including oligopeptides, protein fragments, and growth factors. We have demonstrated patterning in 2D by using photomasks and optical filters to produce both binary and gradient patterns, respectively, and in 3D through a previously developed multiphoton uncaging technique. In addition, we have demonstrated the capacity of our patterning platform to control cell behavior through the alteration of cell morphology, viability, and proliferation. Finally, we have demonstrated the ability to modify the microenvironment of cells in situ without cell damage. We believe that the HyPER platform will provide an invaluable tool for future studies of cell biology and tissue engineering.

Experimental Section

Materials: Hyaluronic acid (60 000 Da, Genzyme Corporation, Cambridge, MA, USA). Adipic dihydrazide, NHS-acrylate, acryloyl chloride, triethylamine, *N*-Boc-ethylenediamine, 4-(4,6-dimethoxy-[1,3,5]triazin-2-yl)-4-methylmorpholinium chloride (DMTMM), vanillin, potassium carbonate, ethyl-4-bromobutyrate, dimethylformamide, nitric acid, ethanol, sulfuric acid, trifluoroacetic acid, methanol, and acetic acid were purchased from Fisher Scientific (Waltham, MA, USA) and used without purification. Picoline borane complex and PEG dithiol ($M_w = 1000$ Da) were purchased from Sigma Aldrich and used without purification. Ac-FKGGGERC-NH$_2$ (K peptide), Ac-GCRDGPQGIWGQDRCG-NH$_2$, NQEQVSPLRGDSPG-NH$_2$ (Q-RGD peptide), and FITC-labeled NQEQVSPLRGDSPG-NH$_2$ were purchased from Genscript (Piscataway, NJ, USA) and used without purification. Four-arm PEG-vinylsulfone (PEG-VS, $M_w = 40$ kDa) and four-arm PEG-maleimide (PEG-MAL, $M_w = 20$ kDa) were purchased from JenKem Technology Inc. (Allen, TX, USA) and used without further purification.

Cell culture: Mouse mesenchymal stem cells (mMSCs, ATCC, cat. no. CRL-12424) were used between P3 and P6. Human umbilical vein endothelial cells (HUVECs, Lonza, cat. no. CC-2519) were used between P3 and P5. Both cell lines were maintained according to the manufacturer's protocols.

ortho-Nitrobenzyl intermediate synthesis

Ethyl 4-(4-formyl-2-methoxyphenoxy)butanoate: Vanillin (20.0 g, 131 mmol), potassium carbonate (36.3 g, 263 mmol), and ethyl-4-

bromobutyrate (25.2 g, 129 mmol) were dissolved in DMF (100 mL), and the mixture was stirred overnight. The solution was precipitated into water (2 L), and the mixture was stirred for 2 h. The resultant precipitate was filtered and washed with water to collect the product (32.6 g, 123 mmol, 95%) as a white powder. ^{1}H NMR (CDCl$_3$): $\delta = 9.89$ (s, 1 H), 7.45 (d, 1 H), 7.42 (s, 1 H), 6.99 (d, 1 H), 4.21 (t, 2 H), 4.19 (q, 2 H), 3.96 (s, 3 H), 2.58 (t, 2 H), 2.18 (m, 2 H), 1.24 ppm (t, 3 H).

Ethyl 4-(4-formyl-2-methoxy-5-nitrophenoxy)butanoate: Nitric acid (70%, 40 mL) was cooled to 0 °C in an ice bath, and ethyl 4-(4-acetyl-2-methoxyphenoxy)butanoate (4.0 g, 15.0 mmol) was added over 5 min. The ice bath was removed, and the solution was allowed to warm to room temperature and react for 3 h. The solution was then precipitated into water and filtered. To purify the product the yellow precipitate was esterified with refluxing ethanol (100 mL) and sulfuric acid (cat.) until TLC (DCM/EtOAc 9:1) indicated that the product was completely esterified. The solution was then allowed to cool slowly and recrystallize. The resulting pale yellow crystals were filtered to give a yield of 3.50 g (11.3 mmol, 75%). ^{1}H NMR (CDCl$_3$): $\delta = 10.50$ (s, 1 H), 7.67 (s, 1 H), 7.45 (s, 1 H), 4.25 (t, 2 H), 4.20 (q, 2 H), 4.03 (s, 3 H), 2.58 (t, 2 H), 2.18 (m, 2 H), 1.24 (t, 3 H).

4-(4-Formyl-2-methoxy-5-nitrophenoxy)butanoic acid: Ethyl 4-(4-formyl-2-methoxy-5-nitrophenoxy)butanoate (5.75 g, 18.4 mmol) was heated to 90 °C in a solution of trifluoroacetic acid (5 mL) and water (50 mL) for 3 h. Once TLC (DCM/EtOAc 9:1) showed complete hydrolysis, the solution was allowed to cool slowly; this resulted in yellow crystals that did not require further purification, beyond filtration (4.49 g, 15.7 mmol, 86%). ^{1}H NMR (300 MHz, [D]DMSO; Figure S2): $\delta = 12.13$ (s, 1 H), 10.14 (s, 1 H), 7.65 (s, 1 H), 7.29 (s, 1 H), 4.20 (t, 2 H), 3.94 (s, 3 H), 2.39 (t, 2 H), 1.98 ppm (m, 2 H).

Caged K peptide synthesis

Photocaging of K peptide: Ac-FKGGGERC-NH$_2$ (30 mg, 33.6 µmol), 4-(4-formyl-2-methoxy-5-nitrophenoxy)butanoic acid (28.5 mg, 101 µmol), and picoline borane complex (8.2 mg, 36.9 µmol) were dissolved in methanol/acetic acid (1.50 mL, 9:1, *v/v*), and the solution was allowed to react for 18 h at room temperature. The product was isolated by preparatory HPLC, eluting with an acetonitrile/water (0.1% TFA) gradient of 5:95→95:5% over 30 min (elution time: 15–17 min). The product was then lyophilized and evaluated with Ellman's reagent (Thermo Scientific–Pierce) to determine product yield, and tested by electrospray mass spectrometry (Waters LCT Premier XE time of flight instrument controlled by MassLynx 4.1 software) to determine purity (see Figure S3). The K* peptide was collected as a pale yellow powder (13.0 µmol, 48% yield).

Synthesis of acrylated hyaluronic Acid (HA-AC)

N-Acryloyl ethylene diamine: Acryloyl chloride (3.03 mL, 37.4 mmol) and chloroform (74.8 mL) were added to a round-bottomed flask equipped with a stir bar under Ar, and the flask was cooled in an ice-water bath. *N*-Boc-ethylenediamine (5.00 g, 31.2 mmol), triethylamine (4.57 mL, 32.8 mmol), and chloroform (37.4 mL) were added dropwise. The mixture was allowed to warm to RT over 2 h, and the chloroform was removed by rotary evaporation. Water (50 mL) was added, and the solution was mixed thoroughly and extracted with chloroform (3×30 mL). The mixture was dried over magnesium sulfate and filtered, and the chloroform was removed by rotary evaporation. The resultant precipitate was dissolved in HCl (7 mL, ~2 mL g^{-1}), and the solution was stirred for 1 h, then placed under

vacuum overnight to evaporate the HCl. The resultant viscous liquid was diluted with ethanol (250 mL) and stirred for 1 h. Precipitates were removed by filtration, and the ethanol was removed by rotary evaporation. Yield: 1.78 g (11.83 mmol, 38%); ^{1}H NMR ([D]DMSO): $\delta = 6.20$ (m, 1H), 6.08 (d, 1H), 5.55 (d, 1H), 3.35 (m, 2H), 2.85 ppm (m, 2H).

HA-AC: Following a modified literature procedure,[20] HA (2.2 g, 5.8 mmol) was dissolved in MES (100 mM, pH 5.5). Following dissolution DMTMM (3.42 g, 11.6 mmol) and *N*-acryloyl ethylene diamine (1.75 g, 11.6 mmol) were added, reacted overnight at RT, and dialyzed with water for 24 h (4×4 L). The resulting solution was lyophilized to achieve the dried product. Yield: 2.1 g (90% yield; 64.45% acrylate modification). The AC modification was characterized by ^{1}H NMR by summing the integration of the three acrylate peaks (^{1}H NMR (D$_2$O): $\delta = 6.20$ (m, 1H), 6.08 (d, 1H), 5.55 ppm (d, 1H)) and dividing by the integration of the HA acetyl peak ($\delta = 1.85$–1.95 ppm (s, 3H).

Degradation kinetics experiment

K* photodegradation kinetics: A stock solution of the K* peptide (0.2 mM) was made in phosphate-buffered saline (PBS). For each time-of-exposure data point ($N = 3$), using a pipette, we placed a spot (0.7 mL) of this solution between two glass slides separated by 0.25 mm spacers. The solution was then exposed to a 20 mW cm^{-2} UV light (Irgacure Series 1000, 365 nm internal band-pass filter) for a predetermined period of time. Following exposure, the solution was testing with trinitrobenzosulfonic acid (TNBSA) according to the protocol published by Pierce Thermo Scientific. The results were analyzed by using Prism software (Graph-Pad Software, Inc.) to determine k [Eq. (1)].

Hydrogel synthesis techniques

Hydrogel type A (nonclustered) synthesis: Lyophilized acrylated hyaluronic acid (HA-AC method 2; 64.45% acrylate modification) was dissolved (0.08 mg μL^{-1}) in triethanolamine (TEOA, 0.3 M, Fisher Scientific) with brief vortexing. K* peptide (0.1 μmol) was dissolved in HA-AC (25 μL, 0.08 mg μL^{-1}) and allowed to react for 20 min at 37°C. TEOA (37.1 μL) and Factor XIIIa (2.78 μL, 180 U mL^{-1}) were added to the solution. This solution was then added to an aliquot of MMP crosslinker (1.07 mg, Ac-GCRDGPQGIWGQDRCG-NH$_2$), and the mixture was briefly vortexed, spotted (10 μL) between two Sigmacote (Sigma–Aldrich) surface-functionalized glass coverslips and placed in an incubator for 45 min at 37°C to gel. (Note: for best results, after all the gel components have been mixed, the pH of the solution should be between 7.9 and 8.2.) Following gelation, the hydrogels were equilibrated in PBS with CaCl$_2$ (0.9 mM).

Hydrogel type B (clustered) synthesis: Lyophilized acrylated hyaluronic acid (HA-AC method 2; 64.45% acrylate modification) was dissolved (0.08 mg μL^{-1}) in TEOA (0.3 M, pH 9.2) by briefly vortexing. K* peptide (0.1 μmol) was dissolved in HA-AC (1.71 μL, 0.08 mg μL^{-1}) and TEOA (22.2 μL), and the mixture was allowed to react for 45 min at 37°C. HA-AC (23.29 μL 0.08 mg μL^{-1}) and Factor XIIIa (2.78 μL 180 U mL^{-1}) were added to this solution, which was then added to an aliquot of MMP crosslinker (1.07 mg, Ac-GCRDGPQGIWGQDRCG-NH$_2$). The mixture was vortexed, spotted (10 μL) between two Sigmacote coverslips and placed in an incubator for 45 min at 37°C to gel (pH 7.9–8.2). Following gelation, the hydrogels were equilibrated in PBS with CaCl$_2$ (0.9 mM).

Hydrogel type C (PEG) synthesis: PEG-MAL, RGD, and K* peptide were dissolved in PBS by briefly vortexing to give stock solutions of 10, 5, and 5 mM, respectively. For a typical gel (15 μL, 2 mM (4 wt%) PEG-MAL and 1 mM of each oligopeptide), aliquots of

each oligopeptide stock (3 μL) and of PEG-MAL stock (3 μL) were combined and allowed to react for 5 min at 37°C. The remaining PBS (4.40 μL) was then added to reach the desired final concentrations. A MMP crosslinker (Ac-GCRDGPQGIWGQDRCG-NH$_2$) was dissolved in PBS to a stock concentration of 28.2 mM. The MMP crosslinker stock (1.60 μL) was added according to the desired r ratio (thiol/maleimide) of 0.75 (3 mM MMP crosslinker) and briefly vortexed, and gel (15 μL) was spotted quickly between Sigmacote coverslips separated by 1 mm spacers and placed in an incubator for 10 min at 37°C to gel. The gels were swelled overnight in PBS (0.9 mM CaCl$_2$).

Note: For acrylate-thiol and vinylsulfone-thiol Michael addition, we found the efficiency of the reaction to be approximately 80%. For example, for 2 mM peptide incorporated into the gelling procedure, we expected 1.6 mM attached peptide due to a competing disulfide formation reaction (with the remainder washing out of the gel through diffusion).

Enzymatic immobilization experiment

Enzymatic attachment quantification: K*-hydrogels (hydrogel type A) were synthesized as described above ($N = 12$). The hydrogels were split into three groups dependent on exposure to 10 mW cm^{-2} UV light (Omnicure Series 1000, 365 nm internal band-pass filter). A fully caged set (negative control) was not exposed; a fully uncaged set (positive control) was exposed for 30 min; and a partially uncaged set was exposed for 5 min. The hydrogels were then exposed to a solution of FITC-labeled Q-RGD in Tris-buffered saline (1 mM, 50 mM CaCl$_2$, 1 U mL^{-1} thrombin) for 3 h. The fractional change in fluorescence for the surrounding solution (compared to the set without K peptide) was used to determine the immobilized fraction.

Predicting immobilization with Equation (1): To predict the expected Q-RGD immobilized shown in Figure 1 D, we first determined the theoretical uncaged fraction by using Equation (1) with $k = 0.24 \times 10^{-4}$ mW^{-1} cm^2 s^{-1} (used for Figure 1 C), $I = 10$ mW cm^{-2}, and $t = 417$ s. We then multiplied the theoretical uncaged fraction (0.5 for this example) by the concentration of Q-RGD immobilized for the fully deprotected sample ((446 ± 85) μM) to provide the expected concentration for the partially uncaged sample ((0.223 ± 42) μM).

General patterning technique used for Figure 2

UV single-photon patterning: Hydrogels (type A for images 2 C–F, type C for 2 B) were placed directly onto a photomasked surface. An Omnicure 1000 mercury vapor lamp (EXFO) equipped with an internal 365 nm narrow band-pass filter delivered UV light (10 mW cm^{-2}) for 10 min to achieve patterned K*-deprotection through the photomask. Light intensity was measured with a UVX digital radiometer (UVP). To create immobilized gradients, a reverse bulls-eye filter (Edmund Optics) was used in place of a photomask.

Confocal multiphoton patterning: We used a modified published protocol to pattern the hydrogels (type A) by multiphoton exposure.[5c] Briefly, a Zeiss confocal CTR MIC microscope was used to create specific designed voids within hydrogels. Regions of interest were drawn within the confocal software for scanning by using a multiphoton laser with a 40× oil-immersion objective (730 nm, intensity setting = 20, 40 scans).

Alexa Fluor 555 staining (Figure 2B): Following patterning, hydrogels (gel type C) were incubated in a solution of NHS-Alexa 555 (10 μg mL^{-1}, succinimidyl ester Alexa 555, Invitrogen) for 2 hours, washed overnight in 1×PBS, and imaged on a Zeiss confocal CTR MIC microscope.

Peptide and protein immobilization: Following patterning, hydrogels (gel types A and B for Figures 2 and 3, respectively) were exposed to conjugation solution (10 μL, 4 mM Q-functionalized peptide or 100 μg mL^{-1} Q-functionalized protein, PBS, 0.9 mM CaCl$_2$) for 3 h at 37 °C. The hydrogels then washed with PBS until background fluorescence was removed.

Q-RGD patterning for controlling mMSC morphology

Hydrogel preparation: Hydrogels were synthesized as described above (gel type B) except that no FXIIIa was included within the gel (FXIIIa was included with the Q-RGD immobilization solution), and the MMP crosslinker was exchanged for a solution of PEG di-thiol (7.31 μL, 0.2 mg μL^{-1}; M_w = 1000 Da, Sigma Aldrich) with the excess volume being subtracted from extra TEOA. Two sets were left caged, two were uncaged (671 s or 80 % theoretical uncaging), and one set was patterned with 100 μm circles. Only one of each caged and fully uncaged set (and the patterned set) was exposed to a Q-RGD (NQEQVSPLRGDSP, 10 % FITC-labeled) conjugation solution following the previously mentioned peptide patterning technique. This resulted in three negative gel sets (+UV/−Q-RGD, −UV/+Q-RGD, and −UV/−Q-RGD) and one positive (+UV/+Q-RGD). In addition, a positive control (synthesized according to the gel type C protocol with 1.6 mM Ac-GCREGRGDSPG-NH$_2$ instead of 1.6 mM K* peptide) and a negative control (synthesized according to the gel type C protocol without addition of K* peptide). The hydrogels were washed overnight with PBS (1 mL per gel) before seeding.

Hydrogel seeding: The hydrogels were seeded with a droplet (10 μL) of complete medium (CDMEM, DMEM with 10 % BGS and 0.1 % P/S) with mMSCs (4000 per gel). The cells were allowed to settle for 1 h before the addition of complete medium (0.5 mL) and culturing for 72 h. The cells were then imaged for analysis by using a Zeiss Observer Z1 fluorescent microscope.

Q-VEGF patterning for controlling HUVEC viability and proliferation

Hydrogel preparation: Hydrogels were synthesized as described above (gel type B) with the addition of Ac-GCREGRGDSPG-NH$_2$ (0.2 mM). The following exposure conditions were used (0, 10, 40, and 80 % uncaged; N = 6 per condition). Half of the gels of each condition were placed directly into PBS with CaCl$_2$ (0.9 mM) to act as a negative control (no Q-VEGF). The rest of the hydrogels underwent Q-VEGF immobilization as described above, with the exception that FXIIIa (10 U mL^{-1}) was included with the Q-VEGF. The hydrogels were washed with PBS (1 mL per gel) for 48 h at 5 °C, with solution changes every ~12 h.

Hydrogel seeding: The hydrogels were seeded with HUVECs (4000 per gel) by using a droplet (10 μL) of EBM-2 (Lonza, Basel, Switzerland) supplemented with EGM-2 SingleQuots Kit without VEGF (EGM-2$_{-VEGF}$). The cells were allowed to settle for 1 h before the addition of EGM-2$_{-VEGF}$ (0.5 mL), then cultured for five days. The cells were then imaged at day 5 by using a Zeiss Observer Z1 fluorescent microscope.

Proliferation analysis: Cell proliferation was quantified by using the CyQUANT Cell Proliferation Assay (Life Technologies). The results were analyzed by using Prism software (GraphPad Software, Inc.), and a one-way ANOVA test was used to determine significance.

LIVE/DEAD analysis of Q-RGD patterning procedure

Hydrogel preparation: Hydrogels were synthesized with inclusion of mMSCs (1500 cells per μL) by using PEG-VS. The PEG-VS stock (20 wt %) was dissolved in HEPES buffer (pH 8.2, 0.3 M). A stock so-

lution of caged K peptide (5 mM) and a stock solution of MMP crosslinker (0.05 mg μL^{-1}) were dissolved in PBS. For a typical gel (45 μL), PEG-VS (13.5 μL), caged K peptide (9 μL), Factor XIIIa (10 μL, 100 U mL^{-1}), and MMP crosslinker (6.95 μL) were combined and spotted (10 μL) between glass slides (1 mm spacer). Following 30 min of incubation at 37 °C, the hydrogels were equilibrated and cultured in CDMEM.

Hydrogel patterning and immobilization: Two sets of hydrogels (N = 3) were exposed to 365 nm light (10 mW cm^{-2}) for 600 s, and a third set was left unexposed. One of the exposed sets underwent the peptide immobilization procedure detailed above for Q-RGD. All sets were washed with CDMEM (2 × 1 mL per gel) while being incubated over the following 24 h.

LIVE/DEAD analysis: Following 24 h of incubation, the hydrogels were tested by LIVE/DEAD assay (Life Technologies). Hydrogels were then imaged by using a Zeiss Observer Z1 fluorescent microscope.

PDGF immobilization with encapsulated mMSCs

Hydrogel preparation: Hydrogels (N = 9) were synthesized according to a type A synthesis, except that 30 % of the gel volume consisted of CDMEM (this volume was subtracted from the total TEOA volume added) with cells (5000 cells per μL). Following gelation, the gels were incubated in CDMEM for 24 h.

Hydrogel patterning: One set of hydrogels (N = 3) was exposed to 10 mW cm^{-2} of 365 nm light passed through two stacked Apodizing Reverse Bullseye optical filters (Edmund Optics, 0.04–2.0 OD, 25 mm) for 600 s to produce a theoretical gradient of ~60–10 % uncaged from the inside to the outside of the gel (~4 mm radius). A second set (N = 3) was exposed uniformly to 10 mW cm^{-2} for 600 s (~75 % deprotection), and a third set (N = 3) was left unexposed.

Immobilization and culturing: All three sets were exposed to Q-PDGF (10 μL, 100 μg mL^{-1}, PBS, 0.9 mM CaCl$_2$) according to the above-mentioned protein-immobilization procedure with PBS washes replaced with three CDMEM washes over two days, after which the hydrogels were fixed with 4 % PFA.

Staining and imaging: Fixed hydrogels were stained according to the manufacturer's protocols for rhodamine phalloidin (Life Technologies) and DAPI (Life Technologies) to label cell actin and nuclei, respectively. Hydrogels were then imaged by using a Zeiss Observer Z1 fluorescent microscope.

Acknowledgements

[1] a) M. V. Turturro, M. C. Christenson, J. C. Larson, D. A. Young, E. M. Brey, G. Papavasiliou, *PLoS One* **2013**, *8*, e58897; b) D. O. Freytes, L. Q. Wan, G. Vunjak-Novakovic, *J. Cell. Biochem.* **2009**, *108*, 1047–1058.

[2] a) A. C. Brown, J. A. Rowe, T. H. Barker, *Tissue Eng. Part A* **2011**, *17*, 139–150; b) M. C. Markowski, A. C. Brown, T. H. Barker, *J. Biomed. Mater. Res. Part A* **2012**, *100*, 2119–2127; c) J. Hodde, R. Record, R. Tullius, S. Bady-

lak, *Biomaterials* **2002**, *23*, 1841–1848; d) S. T. Gould, N. J. Darling, K. S. Anseth, *Acta Biomater.* **2012**, *8*, 3201–3209.

[3] a) J. Lam, T. Segura, *Biomaterials* **2013**, *34*, 3938–3947; b) S. J. Bryant, C. R. Nuttelman, K. S. Anseth, *J. Biomater. Sci. Polym. Ed.* **2000**, *11*, 439–457.

[4] S. Gojgini, T. Tokatlian, T. Segura, *Mol. Pharmaceutics* **2011**, *8*, 1582–1591.

[5] a) J. A. Burdick, A. Khademhosseini, R. Langer, *Langmuir* **2004**, *20*, 5153–5156; b) A. M. Kloxin, A. M. Kasko, C. N. Salinas, K. S. Anseth, *Science* **2009**, *324*, 59–63; c) D. Y. Wong, D. R. Griffin, J. Reed, A. M. Kasko, *Macromolecules* **2010**, *43*, 2824–2831; d) R. G. Wylie, S. Ahsan, Y. Aizawa, K. L. Maxwell, C. M. Morshead, M. S. Shoichet, *Nat. Mater.* **2011**, *10*, 799–806.

[6] Z. Gu, Y. Tang, *Lab Chip* **2010**, *10*, 1946–1951.

[7] S. M. Dallabrida, L. A. Falls, D. H. Farrell, *Blood* **2000**, *95*, 2586–2592.

[8] a) J. C. Schense, J. A. Hubbell, *Bioconjugate Chem.* **1999**, *10*, 75–81; b) A. H. Zisch, U. Schenk, J. C. Schense, S. E. Sakiyama-Elbert, J. A. Hubbell, *J. Controlled Release* **2001**, *72*, 101–113; c) M. Ehrbar, S. C. Rizzi, R. G. Schoenmakers, B. S. Miguel, J. A. Hubbell, F. E. Weber, M. P. Lutolf, *Biomacromolecules* **2007**, *8*, 3000–3007; d) B. H. Hu, P. B. Messersmith, *J. Am. Chem. Soc.* **2003**, *125*, 14298–14299.

[9] A. Ichinose, T. Tamaki, N. Aoki, *FEBS Lett.* **1983**, *153*, 369–371.

[10] M. M. Martino, M. Mochizuki, D. A. Rothenfluh, S. A. Rempel, J. A. Hubbell, T. H. Barker, *Biomaterials* **2009**, *30*, 1089–1097.

[11] D. R. Griffin, A. M. Kasko, *J. Am. Chem. Soc.* **2012**, *134*, 13103–13107.

[12] D. R. Griffin, A. M. Kasko, *ACS Macro Lett.* **2012**, *1*, 1330–1334.

[13] J. F. Goodwin, S. Y. Choi, *Clin. Chem.* **1970**, *16*, 24–31.

[14] a) J. A. McCray, D. R. Trentham, *Annu. Rev. Biophys. Biophys. Chem.* **1989**, *18*, 239–270; b) J. W. Walker, G. P. Reid, J. A. McCray, D. R. Trentham, *J. Am. Chem. Soc.* **1988**, *110*, 7170–7177.

[15] Y. Lei, S. Gojgini, J. Lam, T. Segura, *Biomaterials* **2011**, *32*, 39–47.

[16] Y. S. Ng, R. Rohan, M. E. Sunday, D. E. Demello, P. A. D'Amore, *Dev. Dyn.* **2001**, *220*, 112–121.

[17] a) S. McDougall, J. Dallon, J. Sherratt, P. Maini, *Philos. Trans. R. Soc. A* **2006**, *364*, 1385–1405; b) D. L. Steed, *Surg. Clin. North Am.* **1997**, *77*, 575–586.

[18] F. Balkwill, *Nat. Rev. Cancer* **2004**, *4*, 540–550.

[19] A. Tokunaga, T. Oya, Y. Ishii, H. Motomura, C. Nakamura, S. Ishizawa, T. Fujimori, Y. Nabeshima, A. Umezawa, M. Kanamori, T. Kimura, M. Sasahara, *J. Bone Miner. Res.* **2008**, *23*, 1519–1528.

[20] S. C. Owen, S. A. Fisher, R. Y. Tam, C. M. Nimmo, M. S. Shoichet, *Langmuir* **2013**, *29*, 7393–7400.